Renewable Energy, Environment, and Power Quality Journal (REE&PQJ)
ISSN:3020-531X
Volume No.3, July 2025

AI-Driven Detection of Atmospheric Obstructions Using YOLOv10 and Satellite Imagery for PV System Optimization in the GCC

M. B. Danbatta, N. Al-Azri* and N. Al-Rawahi

Department of Mechanical and Industrial Engineering
Sultan Qaboos University
Al-Khoud 123, Muscat (Oman)
e-mail: nalazri@squ.edu.om

Abstract. The performance of solar photovoltaic (PV) systems is highly dependent on environmental conditions, with atmospheric obstructions significantly impacting energy yield. Traditional monitoring methods rely on ground-based sensors and periodic cleaning schedules, which may not effectively address real-time soiling dynamics. This research presents an AI-powered approach using YOLOv10 to label and train satellite imagery for the detection of dust accumulation, cloud cover, and other obstructions affecting solar radiation reaching PV systems. By integrating deep learning with multi-temporal satellite imagery, an automated framework for real-time environmental monitoring of solar farms is feasible. The YOLOv10 model is trained on labelled datasets to accurately classify dust prone regions, atmospheric disturbances, and potential shading effects. The framework enables early detection of solar obstructions, allowing operators to optimize panel-cleaning schedules, mitigate power losses, and enhance overall energy efficiency. By leveraging satellite-based remote sensing and deep learning, this study offers a cost-effective, scalable solution for maintaining optimal solar PV performance. The findings contribute to sustainable energy development in the GCC region, aligning with national renewable energy goals and ensuring long-term operational efficiency of solar infrastructure.

Key words. Photovoltaic, Detection, Renewable Energy, Solar, Forecasting

Nomenclature

AI	Artificial intelligence
PV	Photo Voltaic
GCC	Gulf Cooperation Council
YOLOv10	You Only Look Once -version 10
mAP	Mean Average Precision

1. Introduction

Artificial intelligence (AI) has already proven transformative for photovoltaic (PV) systems, significantly enhancing their efficiency, reliability, and predictive capabilities. AI-driven techniques enable advanced maximum power point tracking, accurate power forecasting, and early fault detection, addressing limitations of traditional systems, particularly in handling unpredictable weather or minimizing manual interventions. These advancements are especially valuable in the Gulf Cooperation Council (GCC) region, where PV systems face harsh environmental conditions such as dust storms and high humidity[1-2]. Integrating satellite imagery into AI models further strengthens these systems by enabling real-time atmospheric monitoring and adaptive energy management, ensuring minimal disruptions and optimized output[3-4].

In the GCC, where renewable energy deployment is central to national sustainability agendas, AI's role in PV optimization aligns well with goals for reducing emissions and diversifying energy sources. However, environmental challenges like dust accumulation and atmospheric particulates continue to hinder power output, impacting PV efficiency. While natural events like rainfall offer temporary benefits such as panel cleaning, they also introduce short-term output variability, necessitating dynamic and intelligent system responses. Here, AI models like YOLOv10, combined with satellite imagery, offer novel solutions for real-time obstruction detection and predictive system control, supporting sustainable planning and resilience [5].

Among the key challenges in implementing AI-based PV optimization in the GCC include data quality, technological limitations, and economic factors. High-resolution, real-time satellite imagery is essential for accurate model predictions, but such datasets can be hard to obtain and maintain. Additionally, deploying deep learning models like YOLOv10 requires robust computational infrastructure and efficient hardware integration, often lacking in remote or resource-constrained areas. Economic constraints and inconsistent policy support further complicate large-scale AI adoption, despite the region's

abundant solar potential and record-low PV tariffs. To address these issues, standardized frameworks, scalable infrastructure, and supportive regulations are necessary [6].

Globally, a variety of approaches have emerged to optimize PV systems using AI. Hybrid energy systems, combining PV with fuel cells and AI-driven optimization, have shown promising results in boosting efficiency and reducing carbon emissions. AI-enhanced techniques ensure optimal energy harvesting under variable conditions. Predictive maintenance models use AI to detect defects and schedule interventions before breakdowns occur, significantly improving system longevity and performance. Integration with smart home systems and secure, remote-controlled PV operations further demonstrates AI's potential to increase energy reliability and resilience [7].

Other methods, such as ground-based sensors and machine learning models, provide accurate atmospheric data for forecasting but face challenges in scalability and adaptability. Deep learning techniques like convolutional neural networks and object detection models including YOLO and U-Net are effective for cloud and dust detection but demand significant computational resources and large training datasets. Hybrid models combining AI with physics-based predictions improve accuracy but are often computationally intensive. Adaptive PV control strategies, driven by real-time obstruction detection, offer promising results but require seamless integration with grid systems and forecasting tools [8].

Despite these advancements, critical gaps persist. Data incompleteness due to equipment degradation or environmental variability can reduce model accuracy. The absence of standardized data formats and communication protocols hinders interoperability between PV components. AI model transparency remains a concern, particularly with complex neural networks whose decision processes are difficult to interpret. Additionally, regulatory frameworks often lag behind technology, limiting widespread adoption. Emerging AI techniques such as transfer learning and edge computing, which could address many of these challenges remain under-utilized.

To maximize the benefits of AI in PV optimization, particularly in the GCC, a holistic approach is essential, combining technological innovation, policy reform, interdisciplinary collaboration, and real-time, scalable AI models. This ensures not only enhanced energy output and system reliability but also long-term alignment with regional sustainability and climate goals [9-11].

2. Methodology

This study presents a structured framework for developing an AI-driven system that utilizes YOLOv10 and Landsat satellite imagery to detect atmospheric obstructions and optimize photovoltaic system performance in the Gulf GCC region as illustrated in Fig. 1. The methodology encompasses six major phases: data acquisition and preprocessing, annotation, model selection and training, evaluation, integration with PV optimization systems, and deployment. To begin, high-resolution satellite images from Landsat 8 and 9 are acquired through platforms like USGS Earth Explorer and Google Earth Engine. The selection of imagery is guided by both temporal and geographic considerations covering several years to capture seasonal variability, and focusing on GCC countries including Saudi Arabia, United Arab Emirates, Oman, Kuwait, Bahrain, and Qatar.

These images include 30 RGB true composite images, which are essential for detecting different types of atmospheric obstructions such as dust storms, cloud formations, and haze. Preprocessing steps such as radiometric and atmospheric correction, resizing, and normalization are performed to enhance image clarity and ensure compatibility with the deep learning model. Additionally, augmentation techniques like rotation, contrast adjustment, and brightness enhancement are applied to diversify the dataset and improve model robustness.

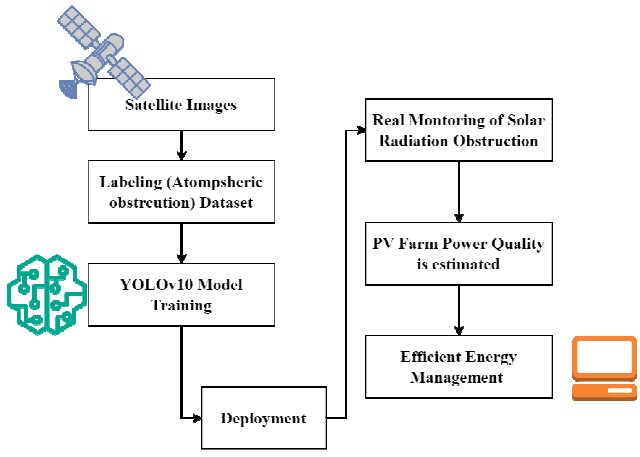

Fig. 1. Overview methodology for using YOLOv10 in satellite imagery dust detection for photovoltaic farms.

Following preprocessing, a comprehensive annotation process was conducted using LabelImg, as illustrated in Fig. 2. Each image was manually labeled with specific obstruction boundary categories: dust, cloud, and ocean. The ocean class was included to minimize false positives in coastal regions, where ocean glare can resemble dust and cloud patterns. In some instances, dust and ocean overlays were observed, especially since most of the image tiles were from coastal areas. The boundaries for dust, cloud, and ocean were manually annotated using LabelImg. Although there was class imbalance dust events being less frequent than cloud and ocean occurrences the selected images primarily featured dust. All annotations were formatted according to YOLO specifications, consisting of bounding boxes and corresponding class labels. YOLOv10 was selected for its high detection accuracy and real-time inference capabilities, making it particularly effective for processing large-scale satellite imagery.

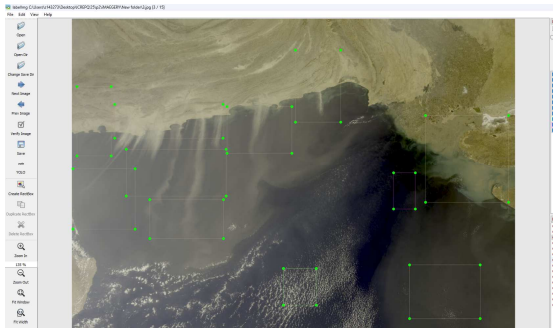

Fig. 2 Sample of Image satellite imagery Annotation process.

The model's advanced architecture featuring spatial-channel decoupled downsampling and a lightweight classification head enables efficient detection of fine-grained features while maintaining low computational overhead. The training process utilizes transfer learning with pre-trained weights, which enhances performance and accelerates convergence. The labeled dataset is split into 80% for training, 10% for validation, and 10% for testing. Key hyperparameters such as learning rate, batch size, and number of epochs are carefully tuned to achieve optimal results. The YOLO model was trained using the following parameter ranges: learning rate between 0.001 and 0.0001, batch size between 16 and 32, and epochs ranging from 1 to 10.

The model is evaluated using a range of metrics to ensure both accuracy and real-world applicability. Mean Average Precision (mAP) is used to assess overall detection performance across all obstruction classes, while Intersection over Union measures the overlap between predicted and ground-truth bounding boxes. Precision and recall help determine the model's balance between false positives and false negatives, and the F1-score provides a comprehensive performance indicator. Real-time detection capabilities are evaluated through inference speed, measured in frames per second, to ensure timely integration with PV system operations.

3. Results and Discussion

The training results of the YOLOv10 model demonstrate a consistent and significant improvement across multiple performance metrics over ten epochs as illustrated in Table 1 and Fig. 3. Initially, the model exhibited high training losses particularly in box loss 3.74, class loss 5.18, and distance from loss 2.84 with zero mAP. This suggests that during the early stages, the model was still learning basic spatial and classification features from the satellite imagery.

Table 1. Training and validation performance metrics across epochs for the developed YOLOv10 model.

Epoch	Train/ Box Loss	Train/ Class Loss	Precision (B)	Recall (B)	mAP50 (B)	mAP50-95 (B)	Val/ Box Loss	Val/ Class Loss
1	3.74	5.18	0.00	0.00	0.00	0.00	3.65	4.59
2	3.44	4.47	0.12	0.13	0.07	0.02	3.18	3.81
3	2.92	3.31	0.52	0.13	0.08	0.02	2.93	4.20
4	2.45	2.76	0.50	0.31	0.18	0.06	2.72	15.6
5	2.16	2.56	0.56	0.40	0.31	0.14	2.27	11.8
6	2.20	2.28	0.57	0.45	0.29	0.18	1.93	5.14
7	1.94	1.83	0.72	0.36	0.28	0.19	1.54	3.51
8	1.50	1.51	0.74	0.44	0.37	0.23	1.43	2.58
9	1.39	1.48	0.77	0.36	0.51	0.28	1.28	2.01
10	1.44	1.42	0.77	0.36	0.57	0.38	1.20	1.77

By the second epoch, although losses remained relatively high, a notable improvement in model confidence emerged, with the precision reaching 11.5% and recall at 13%. This reflects the model beginning to detect some relevant features related to dust, or cloud cover targets identified in the study for optimizing solar PV monitoring using satellite images. By epoch 3, the training loss declined further while precision surged to over 52%, though recall remained static. This indicates the model became more certain in its correct detections, but was still missing many positive cases typical in early stages of deep learning as the model tightens bounding boxes before expanding detection generalization. The turning point appears from epoch 4 onward, with steady decreases in both classification and box losses. Meanwhile, mAP50 improved to over 18% and mAP50-95 began to climb, reflecting better localization and confidence calibration in prediction.

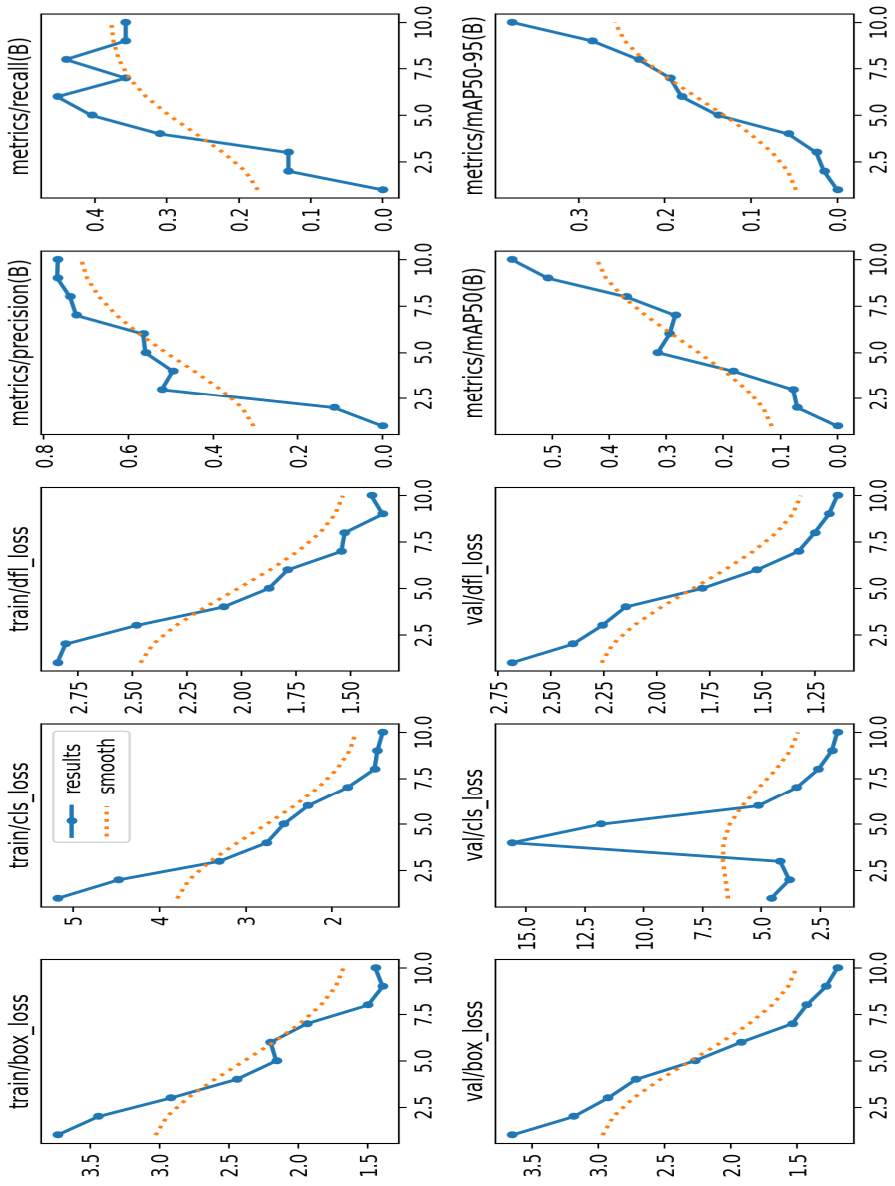

Fig. 3. Model training performance metrics.

This directly supports the framework's goal of identifying soiling and atmospheric disruptions in real-time. From epochs 5 to 7, validation losses dropped significantly, with val-box loss reaching as low as 1.43 and val-class loss improving to under 3.5. The model's recall improved, peaking at 45%, while mAP50 and mAP50-95 steadily climbed. These results indicate improved generalization across unseen satellite data and the model's growing ability to detect environmental features that impact solar performance. By epoch 8, the model showed a marked balance between precision 73.8% and recall 44%, with a notable jump in mAP50 to 37% and mAP50-95 reaching 23%. This performance directly translates to more reliable detection of environmental obstructions, empowering operators to anticipate soiling events and adjust maintenance schedules effectively. In the final epochs 9 and 10, the model reached its highest mAP50 of 57% and mAP50-95 of 37.7%, with validation losses now minimal. These outcomes illustrate that the deep learning pipeline effectively learned complex patterns from temporal satellite data, aligning with the research objective to automate and scale solar farm monitoring in real time. Fig. 4 depicts the precision confidence curve of the model.

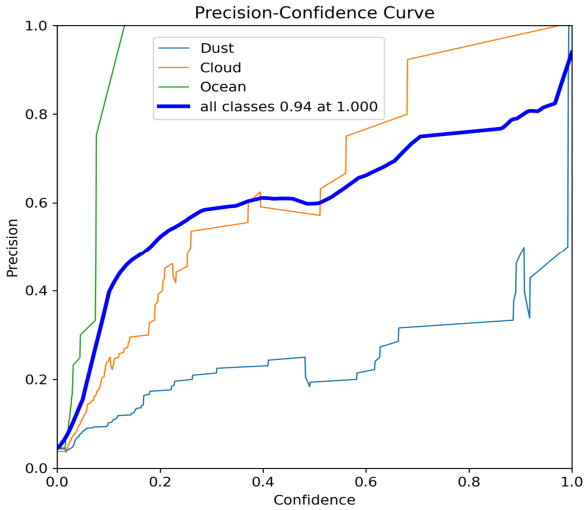

Fig. 4. Precision-confidence curve for YOLOv10 dust detection in satellite images.

Fig. 5 and 6 shows the results of the prediction of the model after training the model. Overall, the YOLOv10 training performance validates its application in environmental monitoring for solar PV systems. The growing accuracy across all metrics reinforces the model's potential in contributing to sustainable energy operations in the GCC. The AI-powered approach not only aligns with national renewable goals but also enhances operational efficiency by detecting real-time obstructions, marking a pivotal advancement in smart solar infrastructure management.

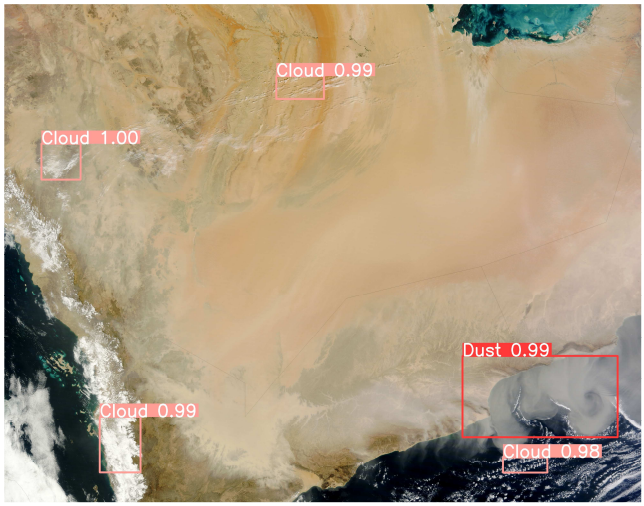

Fig. 5. Prediction result: sample #1 imagery detected objects with bounding boxes, class labels, and confidence scores.

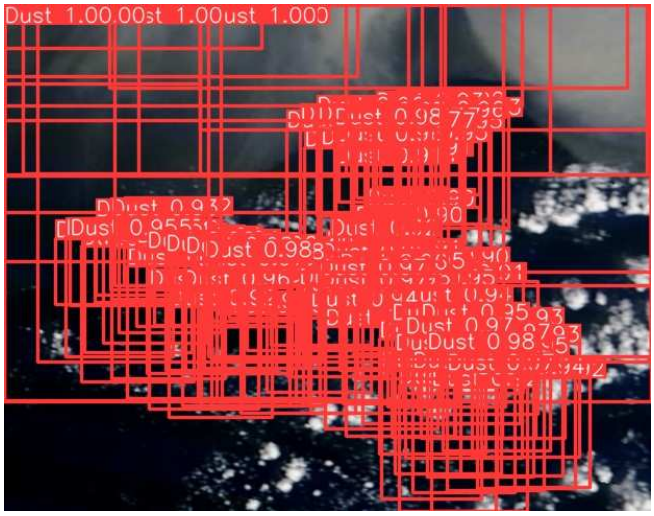

Fig. 5. Prediction result: sample #2 imagery detected objects with bounding boxes, class labels, and confidence scores.

4. Conclusion

The results demonstrate that the YOLOv10-based deep learning framework can effectively detect environmental obstructions such as dust accumulation, cloud cover, and shading, all of which negatively impact the performance of solar PV systems. A progressive improvement in precision, recall, and mean Average Precision over ten training epochs confirms the model's learning efficiency and ability to generalize well across diverse satellite imagery.
The integration of satellite-based remote sensing with real-time, AI-driven analysis has proven to be both scalable and cost-effective, offering a robust alternative to traditional ground-based monitoring systems. This directly supports the study's core objective: enhancing the operational efficiency of solar infrastructure, particularly in the GCC region, where atmospheric conditions frequently disrupt solar energy production.

To overcome data scarcity or limitations in satellite image availability, especially for the GCC, the use of frequent real-time imagery from multiple satellite sources is recommended. Additionally, applying data augmentation techniques can help expand limited datasets and improve model robustness. The model's ability to accurately classify and localize obstructions supports proactive maintenance strategies, enabling optimized cleaning schedules, reduced power losses, and increased overall energy yield. However, the main source of error stems from thin dust and cloud misclassification particularly cirrus clouds, which can resemble dust posing a challenge to precise detection.

To further enhance system performance, future work should incorporate a broader and more diverse dataset, capturing seasonal variations and extreme weather conditions to improve the model's robustness. The current dataset offers limited temporal diversity relative to its size, which may affect the model's ability to generalize across time. Integrating additional environmental variables such as wind speed, humidity, and particulate matter could further refine both detection accuracy and predictive capabilities.

Deploying the trained model within a real-time operational monitoring platform would facilitate continuous feedback and support adaptive learning in the field. Furthermore, expanding the study to encompass geographically diverse regions with varying climatic profiles would help validate the model's generalizability and promote its global scalability. Collectively, these enhancements would solidify the proposed framework as a critical tool in the advancement of smart, sustainable, and efficient solar energy systems.

References

[1] N. Al-Azri, Y. Zurigat and N. Al-Rawahi, "Development of bioclimatic chart for passive building design in Muscat-Omant," Renewable Energy and Power Quality Journal, vol. 10, p. 1809, 2012, doi: https://10.24084/repqj10.841.

[2] M. B. Danbatta, N. Al-Rawahi, and N. Al-Azri, "Satellite-Ground Temperature Correlation for Solar Energy: Insights from Oman," JMCER, vol. 2025, pp. 1–9, 2025.

[3] M. B. Danbatta, N. Al-Azri, and N. Al-Rawahi, "Analysis of Solar Radiation and Remote Sensing Indices for Coastal Management in Oman.," Journal EJENS-European Journal of Engineering & Natural Sciences, vol. 9, no. 1, 2024.

[4] M. Kolahi, S. M. Esmailifar, A. M. Moradi Sizkouhi, and M. Aghaei, "Digital-PV: A digital twin-based platform for autonomous aerial monitoring of large-scale photovoltaic power plants," *Energy Convers Manag*, vol. 321, p. 118963, 2024, doi: https://doi.org/10.1016/j.enconman.2024.118963.

[5] G. B. Balachandran, M. Devisridhivyadharshini, M. E. Ramachandran, and R. Santhiya, "Comparative investigation of imaging techniques, pre-processing and visual fault diagnosis using artificial intelligence models for solar photovoltaic system – A comprehensive review," *Measurement*, vol. 232, p. 114683, 2024, doi: https://doi.org/10.1016/j.measurement.2024.114683.

[6] H. Mao *et al.*, "Advances and prospects on estimating solar photovoltaic installation capacity and potential based on satellite and aerial images," *Renewable and Sustainable Energy Reviews*, vol. 179, p. 113276, 2023, doi: https://doi.org/10.1016/j.rser.2023.113276.

[7] A. Al-Janabi and N. Al-Azri, "Effect of recovering the industrial waste heat in Oman on energy and environment," Energy Reports, vol. 6, p. 526, 2020, doi: https://doi.org/10.1016/j.egyr.2020.11.203.

[8] T. Zhong *et al.*, "Assessment of solar photovoltaic potentials on urban noise barriers using street-view imagery," *Renew Energy*, vol. 168, pp. 181–194, 2021, doi: https://doi.org/10.1016/j.renene.2020.12.044.

[9] S. Zhao, H. Chen, C. Wang, Y. Zhou, and Z. Zhang, "RGR-Net: Refined Graph Reasoning Network for multi-height hotspot defect detection in photovoltaic farms," *Expert Syst Appl*, vol. 245, p. 123034, 2024, doi: https://doi.org/10.1016/j.eswa.2023.123034.

[10] A. Leonard, S. Wheeler, and M. McCulloch, "Power to the people: Applying citizen science and computer vision to home mapping for rural energy access," *International Journal of Applied Earth Observation and Geoinformation*, vol. 108, p. 102748, 2022, doi: https://doi.org/10.1016/j.jag.2022.102748.

[11] M. B. Danbatta, N. Al-Azri, and N. Al-Rawahi, “Exploring the Impact of Solar Radiation on Environmental Dynamics in Oman Normalized Difference Vegetation Index (NDVI),” *European Journal of Engineering and Natural Sciences*, vol. 9, no. 1, pp. 15–19, 2024.